Journal of Glaciology

Article

*Present address: Geological Sciences Building 101, University of Texas at El Paso, 500 W. University Ave., El Paso, TX 79968

Cite this article: Karplus MS et al. (2024). Signal characteristics of surface seismic explosive sources near the West Antarctic Ice Sheet divide. *Journal of Glaciology* **70**, e16, 1–11. https://doi.org/10.1017/jog.2024.41

Received: 4 November 2023
Revised: 27 March 2024
Accepted: 25 April 2024

Keywords:
Glacier geophysics; glaciological instruments and methods; seismics; seismology

Corresponding author:
Marianne Karplus;
Email: mkarplus@utep.edu

cambridge.org/jog

Signal characteristics of surface seismic explosive sources near the West Antarctic Ice Sheet divide

Marianne S. Karplus[1]*, Nori Nakata[2], Galen M. Kaip[1], Steven H. Harder[1], Lucia F. Gonzalez[1], Adam D. Booth[3], Emma C. Smith[3], Stephen A. Veitch[1,4], Jacob I. Walter[5] and Poul Christoffersen[6,7]

[1]Dept. of Earth, Environmental, and Resources Sciences, University of Texas at El Paso, El Paso, TX, USA; [2]Earth, Atmospheric, and Planetary Sciences, Massachussetts Institute of Technology, Cambridge, MA, USA; [3]School of Earth and Environment, University of Leeds, Leeds, AL, USA; [4]Earthscope Consortium, Socorro, NM, USA; [5]School of Geosciences, University of Oklahoma, Norman, OK, USA; [6]Institute for Marine and Antarctic Studies, University of Tasmania, Hobart, TAS, Australia and [7]Australian Centre for Excellence in Antarctic Science, Hobart, TAS, Australia

Abstract

Seismic imaging in 3-D holds great potential for improving our understanding of ice sheet structure and dynamics. Conducting 3-D imaging in remote areas is simplified by using lightweight and logistically straightforward sources. We report results from controlled seismic source tests carried out near the West Antarctic Ice Sheet Divide investigating the characteristics of two types of surface seismic sources, Poulter shots and detonating cord, for use in both 2-D and 3-D seismic surveys on glaciers. Both source types produced strong basal P-wave and S-wave reflections and multiples recorded in three components. The Poulter shots had a higher amplitude for low frequencies (<10 Hz) and comparable amplitude at high frequencies (>50 Hz) relative to the detonating cord. Amplitudes, frequencies, speed of source set-up, and cost all suggested Poulter shots to be the preferred surface source compared to detonating cord for future 2-D and 3-D seismic surveys on glaciers.

1. Introduction

The physical and chemical properties of Antarctic glacial ice and the bed beneath it yield critical information about past and present climate conditions and ice dynamics that can be used to model future scenarios of ice evolution in a changing climate (Pattyn, 1996; Truffer and others, 2001; Pimentel and others, 2010; Sergienko and Hulbe, 2011). Controlled-source seismic reflection profiling is a powerful method that has long been used to determine ice thickness, englacial properties, as well as subglacial hydrology, lithology, and topography (e.g., Bentley and Ostenso, 1961; Roethlisberger, 1972; Blankenship and others, 1987; Booth and others, 2012; Picotti and others, 2015). It has also been important for determining relationships between seismic velocity and density, temperature and crystal orientation fabric (COF) (e.g., Robin, 1953; Bentley, 1972; Kohnen, 1974; Peters and others, 2012). The success and feasibility of controlled-source seismic experiments depend, in part, on selecting seismic sources that satisfy experimental goals while also being compatible with field logistical constraints. Direct comparisons of amplitudes, frequencies, and field set-up procedures for different source types can help scientists select the right source for their imaging project.

Since the 1980s, controlled sources used in Antarctica for imaging ice more than 1-km thick primarily involve setting explosive charges in 15–30 m deep boreholes (Blankenship and others, 1987; Luthra and others, 2016). The borehole approach reduces the effects of strong seismic attenuation in the firn and also reduces the ground roll (surface waves), but it requires specialized and sometimes heavy ice drilling equipment, drilling expertise, and time to drill holes. Borehole shots also result in a secondary 'ghost' reflection from the ice-air interface which travels closely behind the primary package of seismic waves. This can complicate seismic analyses of bed properties because the bed reflection recorded at the surface includes interference of the primary bed reflection and the 'ghost' reflection. Glaciologists typically reduce or remove this interference of the 'ghost' with the primary bed reflection by burying shots at depths (e.g., 20–25 meters) that allow for good separation (30 ms) between the primary and ghost return.

The problems inherent to borehole shots can be overcome using surface explosive sources, such as detonating cord (Sen and others, 1998; Diez and others, 2015; Hofstede and others, 2021), shallow (<5 m depth) drilled shots, or Poulter shots. Poulter shots were originally designed and used in Antarctica for seismic surveys on the Ross Ice Shelf during Byrd's second expedition from 1933–1935 and then became part of standard geophysical practice (Poulter, 1950). Poulter shots involve mounting explosives above the ice sheet surface with the shock wave hitting the surface generating the seismic waves. Explosions at the surface or within the firn create a diving wave by compacting the firn around them. Most energy of a shallow drilled explosion in firn is lost as it travels back to the surface. Surface and shallowly-drilled

https://doi.org/10.1017/jog.2024.41 Published online by Cambridge University Press

explosions as well as other sources appear to benefit from vertical directivity of the source, one reason why sources directed downward such as Poulter shots, detonating cord, and vibroseis work from the surface (Poulter, 1950; Hofstede and others, 2021). For shallower (<1 km) ice thicknesses, hammer strikes, buffalo or Betsy seismic guns, and weight drop sources are also practical ice surface sources (Booth and others, 2013; Veitch and others, 2021). Stacking these sources can sometimes increase signal-to-noise ratios enough to allow imaging of ice more than 1-km thick. On-ice vibroseis sources capable of imaging ice thicknesses typically found in Antarctica are generally large and require significant logistical preparations, but the seismic images can be high quality (Eisen and others, 2015).

In this paper, we report results from controlled seismic source tests carried out in Antarctica investigating the quality of two types of surface seismic sources, Poulter shots and detonating cord, for use in large 2-D and 3-D seismic surveys. We conducted these tests largely to identify optimal seismic sources to use for 3-D seismic imaging across the Eastern Shear Margin of Thwaites Glacier, as part of the Thwaites Interdisciplinary Margin Evolution (TIME) project. The field sites at Thwaites are remote locations where our team will have limited cargo resources and limited field time, so we require lightweight and quick-to-setup seismic sources with strong, isotropic signals and frequency content that allow imaging and characterization of the $\sim 2-2.5$ km of ice and the glacier bed below.

We tested the surface seismic sources ~5 km northeast of the West Antarctica Ice Sheet (WAIS) Divide Camp of the U.S. Antarctic Program, during January 2019. WAIS Divide Camp (S 79.467°, W 112.085°) is located at 1766 meters height above the WGS-84 ellipsoid and about 24 km from the ice flow divide, which separates the region where the ice flows to the Ross Sea from the region where ice flows to the Amundsen Sea (Conway and Rasmussen, 2009). The current ice accumulation rate is 22 cm/ year, the average annual surface temperature is −30°C, and the ice thickness is 3465 meters. The bubble close-off depth at WAIS Divide is 67–77 meters (Battle and others, 2011).

We selected the location for the source testing to avoid noise coming from WAIS Divide Camp and to align with a controlled-source seismic line that was collected during the 2008-2009 season (Horgan and others, 2011). We chose to conduct our seismic sources tests in the same location to allow the possibility of comparison with the drilled shots (24 meters depth) used in that survey. The profiles extended ~2.5 km (2009) and ~3.25 km (2019) along-flow towards the Walgreen Coast (Amundsen Sea sector). The selected testing location has the added benefit of the potential to compare the ice structure and fabric derived from our seismic survey to the structure and fabric seen in the WAIS Divide ice core (Kluskiewicz and others, 2017). Our seismic line is also partially co-located with a radar line collected in 2020 (Young and others, 2021). Several recent studies used passive seismic data collected during the 2019 source testing to investigate detailed wave propagation in firn (Chaput and others, 2022a, 2022b, 2023) and shallow ice sheet composite structure (Zhang and others, 2022).

This shot testing provides valuable comparisons of surface shot effectiveness for 2-D and 3-D surveys of glacial environments with up to 3-km-thick ice. We tested multiple different configurations of Poulter shots and multiple configurations of detonating cord to observe the signal quality, frequency content, and anisotropy of seismic waves radiating from the different configurations. We also tested near-surface shots with explosives placed in shallow holes, less than 5 meter depth. Poulter shot variations included type, height above snow surface, and quantity of explosive. Detonating cord variations included thickness of cord, amount of cord, and geometric arrangement of the cord. In this paper, we summarize the results regarding the benefits and limitations of surface seismic sources in glacial environments.

2. Seismic source testing field methods

The seismic tests were conducted in January 2019 along a 3.25-km-long line located ~5 km northeast of WAIS Divide Camp and oriented along the ice flow direction, toward the Walgreen Coast (Fig. 1). The test shots were made at three shot points along the 3.25-km-long line (Fig. 1). Shotpoint 1 (0 km offset) and shotpoint 3 (3.25 km offset) were off ends of the main receiver line, and shotpoint 2 (1.625 km offset) was in the middle of the receiver line. The shots were recorded on a combination of 100 Magseis Fairfield Z-Land Generation 2, 5-Hz, 3-component seismic nodes (Ringler and others, 2018) and a 48-channel cabled Geometrics Geode system using 4.5-Hz geophones. The recording system was configured into 3 arrays, as follows: Array 1 consisted of a 2.25-km-long line of 75 nodes at 30-m spacing, with the first node at 0.5 km offset and the last at 2.75-km offset; Array 2 consisted of 24 nodes in a 0.5 km radius circle, centered around shotpoint 1 (0 m offset); Array 3 was a 235-meter-long line of 48 geophones at 5-m intervals between 0.265 km and 0.5 km offsets.

Nodes were buried at 30 cm depth, leveled with a bubble level, and oriented using an Antarctica-weighted Brunton compass. Nodes were programed with a sampling rate of 1000 Hz, a pre-amp gain of 12 dB, a linear phase Nyquist filter, and DC offset removal. The seismic nodes recorded continuously for the entire experiment. The first nodes were deployed on January 6, 2019, and the nodes were retrieved on January 15, 2019. Node data were merged into a PH5 volume by the Earthscope Primary Instrument Center and archived at the Earthscope Data Management Center as network 2E 2018 and assembled dataset 18–030 (Kaip and others, 2018). The geophones remained in the same configuration during all of the shots discussed in this paper. Geode data were saved in SEG2 format and converted to SEGY for analysis. The Geode cabled seismic system recorded from 1 second before the minute to 15 seconds after each minute. Sources were fired on the minute using a GPS clock, a seven Joule shooting system, DaveySeis electronic detonators, and a Davey Bickford Universal Seismic Interface. For safety reasons, we always use electronic detonators (instead of electric detonators) to fire surface explosives. Shots were detonated on days with relatively low wind and calm weather. Figure 2 contains photos and schematic diagrams of several types of sources tested.

Twenty six surface sources were detonated at shotpoint 1, with nine different configurations of Poulter shots, comprised of different amounts, heights and types of explosives (Table 1) and seventeen different configurations of detonating cord shots (Table 2). The detonating cord was arranged in various patterns such as lines, crosses, and swirls at the snow surface and covered with a small amount of snow to weigh down the cord (Table 2). Fifteen surface sources were detonated at shotpoint 2 including four different configurations of Poulter shots and eleven different configurations of detonating cord (Tables S1, S2). Nine surface sources were detonated at shotpoint 3 including four different configurations of Poulter shots and five different configurations of detonating cord (Tables S4, S5). At each of the three shotpoint locations, we also detonated two 150-gram pentolite boosters loaded at 2.3 to 3.4 m depth in a shot hole drilled by a 4-meter Kovacs ice auger (Tables 3, S3, S6). Similar shots were also made at 37 additional locations along the line, with 60-m spacing, in between almost every other pair of nodes (Fig. 1). These data are incorporated in other papers focused on controlled-source seismic imaging (e.g., Zhang *et al.*, in prep.).

For the Poulter shooting we used a custom-designed Poulter shot pole to suspend explosives at heights of 1.83 to 2.44 m (6 ft and 8 ft, respectively) above the snow surface. The pole design consisted of a 6.35 by 6.35 cm square telescoping aluminum pole, that extended up to 1.52 m. A ~1 m long piece of

https://doi.org/10.1017/jog.2024.41 Published online by Cambridge University Press

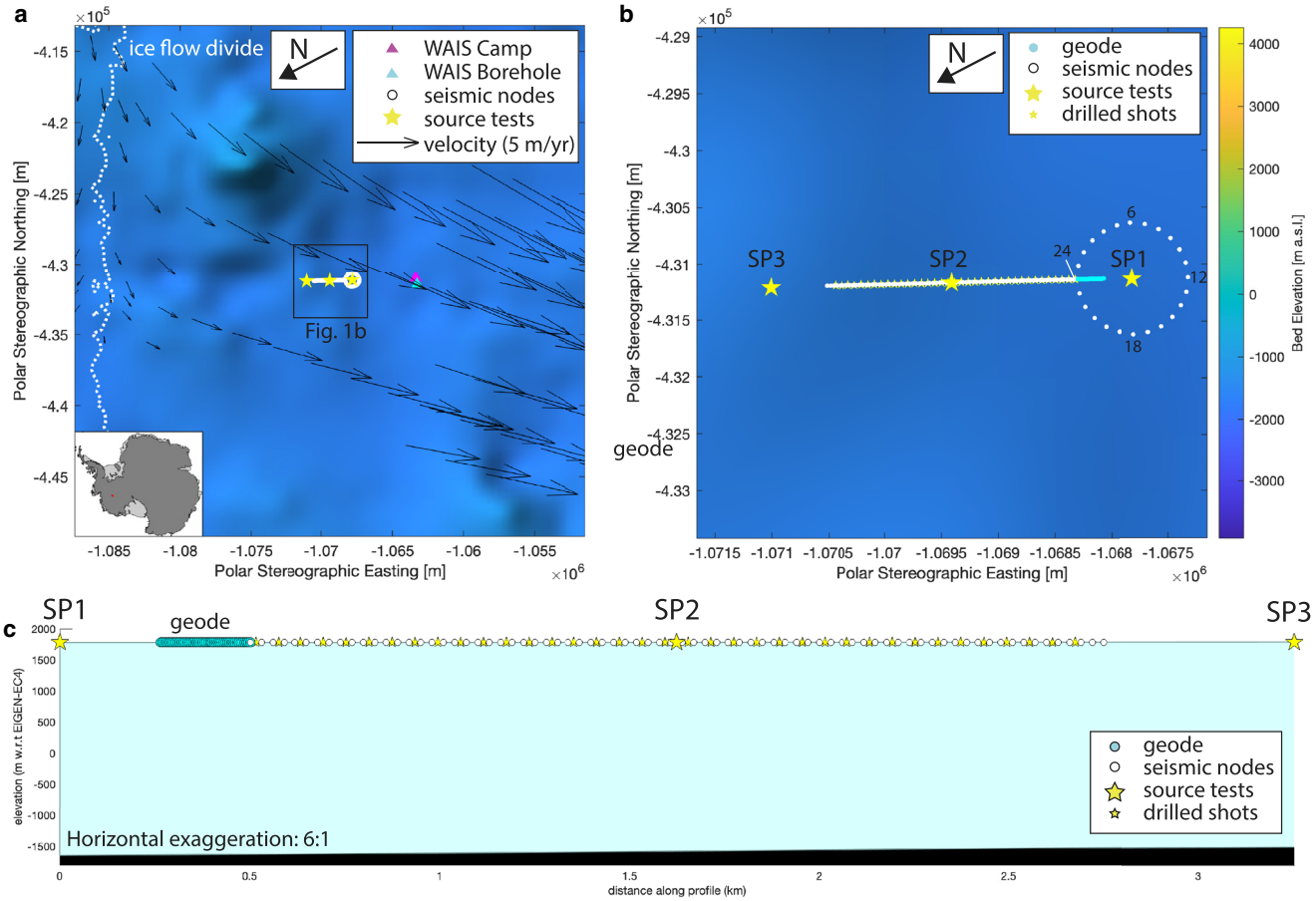

Figure 1. Location maps for surface seismic source testing near West Antarctic Ice Sheet (WAIS) Divide. (a) Map showing location of the seismic test site ~5-km northeast of WAIS Divide Camp. Bed elevation is from BedMachine v3 (Morlighem and others, 2020). Arrows show the ice flow measured near WAIS Divide (Conway and Rasmussen, 2009). Dashed white lines show the location of the ice flow divide. Ice southwest of the divide flows toward the Ross Sea, and ice northeast of the divide flows toward the Amundsen Sea. (b) Zoomed in map of the seismic line and locations of sources and receivers used for shot testing. Maps were plotted in MATLAB using Antarctic Mapping Tools (Greene and others, 2017). Numbers indicate trace or node numbers for nodes in the circle. These numbers are used in Figures 3–5 for numbering the node circle traces. (c) Horizontally exaggerated (6:1) cross section along the line from shotpoint (SP) 1 to 3 showing locations of sources and receivers and bed depths from BedMachine v3 (Morlighem and others, 2020).

sacrificial wood (1.27 by 1.91 cm) was attached to the top, and the explosives were fastened to the wood with cold-resistant tape (Fig. 2) at the desired heights (either 1.83 to 2.44 m). We detonated dynamite (extra gelatin nitrogylcerin dynamite, Unimax brand name), emulsion blasting agent (booster sensitive emulsion, Blastex brand name), and pentolite boosters (Powerplus P brand name), with total explosive weights of 2.5 kg, 4 kg, 5 kg, and 5.4 kg (Table 1). Detonating cord products included both 10.8 grams per meter (50 grains per foot) and 85 grams per meter (400 grain per foot) cord (Table 2). Linear configurations included lines with length 16.4 m (0.18 kg) oriented inline with the receiver line and perpendicular to the receiver line. Swirl configurations included swirls with length 16.4 m (diameter 3 m; 10.8 g/m: 0.18 kg; 85 g/m: 1.39 kg), 20.4 m (diameter 3.5 m;

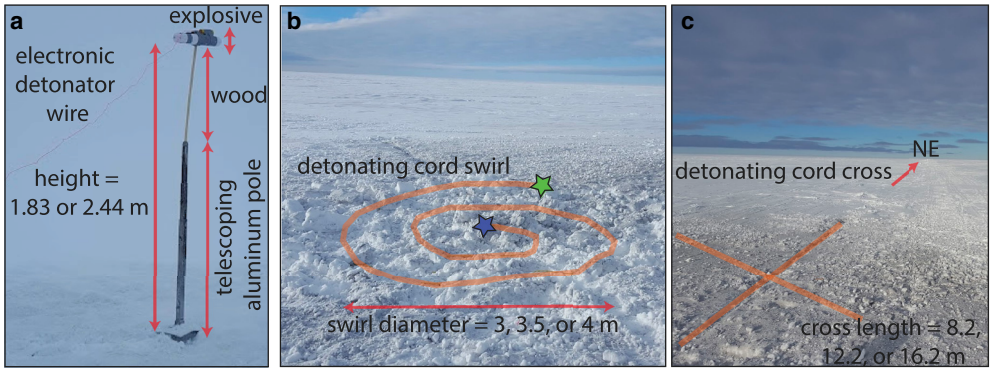

Figure 2. Example surface source configurations tested near West Antarctic Ice Sheet Divide camp. (a) Photo of an example Poulter shot, shot 5044, labeled with telescoping aluminum pole, sacrificial wood, explosive, and electronic detonator wire. Explosives included 5 kg emulsion plus 400 g pentolite booster detonated at 2.44 m above the snow surface. (b) Photo of an example detonating cord swirl, shot 5035. The detonating cord is partially weighed down with snow, so the cord location is highlighted in orange. This swirl used 32.4 m 10.8 g/m cord with a 3 m diameter, and the swirl was fired inside-out. Green star: location of detonator for outside-in shooting; blue star: location of detonator for inside-out shooting. (c). Schematic diagram of a detonating cord cross overlain on a picture of the field environment. The lines of the cross were oriented parallel (northeast) and perpendicular to the direction of the seismic line. Figures 2a–c do not have the same length scales.

https://doi.org/10.1017/jog.2024.41 Published online by Cambridge University Press

Table 1. Poulter explosive source descriptions for sources fired at shotpoint 1 as part of source testing near West Antarctic Ice Sheet (WAIS) Divide

Shot ID	Weight (kg)	Height (m)	Type	Description
5001	5.0	2.44	Dynamite	2 – –75 × 400 mm charges
5002	2.5	2.44	Dynamite	1 – 75 × 400 mm charge
5003	5.4	2.44	5 kg emulsion + 400 g pentolite booster	2 – 75 × 400 mm charges +400 g booster
5004	4.0	2.44	10 400 g pentolite booster	10 boosters taped on horizontal wood
5005	5.0	1.83	Dynamite	2 – 75 × 400 mm charge
5006	5.0	1.83	Dynamite	2 – 75 × 400 mm charge
5007	2.5	1.83	Dynamite	1 – 75 × 400 mm charge
5008	5.4	1.83	5 kg emulsion +400 g pentolite booster	2 – 75 × 400 mm charge +400 g booster
5009	4.0	1.83	10 400 g pentolite booster	10 boosters taped on horizontal wood

10.8 g/m: 0.22 kg; 85 g/m: 1.73 kg), and 32.4 m (diameter 4 m; 10.8 g/m: 0.35 kg; 85 g/m: 2.75 kg). Swirls were fired inside-out (detonator in middle of swirl) and outside-in (detonator on outside branch of swirl). Cross configurations included lengths of 8.2 m (0.09 kg), 12.2 m (0.13 kg), and 16.2 m (0.17 kg) for each branch of the cross. The crosses included two linear cords with one parallel to the receiver line and one perpendicular to the receiver line.

As well as the source characterization discussed in the paper, the passive seismic data recorded by these arrays has allowed characterization of ambient high frequency seismic wavefields in the firn column (Chaput and others, 2022a), near-surface seismic anisotropy (Chaput and others, 2022b), and estimation of shear-wave velocities as well as imaging of an englacial reflector from seismic wavefield imaging (Zhang and others, 2022).

3. Comparisons of Poulter, detonating cord, and shallow drilled shots

For each of the various source types, the recorded waveforms (including amplitudes, times, and frequencies) were examined. Shot gathers for Poulter shot 5004 (4 kg of pentolite boosters suspended at 2.44 m above the ice) recorded on array 1 and array 2 show clear P-wave, S-wave, surface wave, and air wave arrivals (Fig. 3). There is also a clear P-wave arrival at ∼1.7 − 1.8 seconds that we interpret as a bed reflection. A multiple of the bed reflection is seen clearly at ∼3.5 seconds (Fig. S1). The air wave recorded by array 2 has variable travel times across the circle, most likely due to the impact of wind speed on the speed of sound of the detonation (Fig. 3). Shot gathers for detonating cord shot 5026 (swirl using 32.4 m of 85 g/m detonating cord, fired inside-out with 4 m diameter, 2.75 kg explosive) recorded on array 1 and array 2 also show clear P-wave, S-wave, surface wave, and air wave arrivals (Fig. 4). We see the same, clear P-wave bed reflection at ∼1.7 − 1.8 seconds. A multiple of the bed reflection is seen clearly at ∼3.5 seconds (Fig. S2, S3). The air wave recorded by array 2 is also impacted by wind speed and direction (Fig. 4). As expected, the vertical component contains the strongest signal, followed by the radial component, and the transverse component has a less clear signal. Shot gathers for shallow drilled shot 5053, with two 150-g pentolite boosters buried at 3.1 meters depth, are noisier but also show P-wave, S-wave, surface wave, and air wave arrivals (Fig. S4).

Table 2. Detonating cord explosive source descriptions for sources fired at shotpoint 1 as part of source testing near West Antarctic Ice Sheet (WAIS) Divide

Shot ID	Weight (kg)	Length (m)	Type	Shape	Description
5010	0.18	16.4	10.8 g/m	line	Parallel to receiver line
5011	0.18	16.4	10.8 g/m	line	Perpendicular to receiver line
5012	0.18	16.4	10.8 g/m	swirl	Fired inside-out
5013	0.22	20.4	10.8 g/m	swirl	Fired inside-out
5014	0.35	32.4	10.8 g/m	swirl	Fired inside-out
5015	0.18	16.4	10.8 g/m	swirl	Fired outside-in
5016	0.22	20.4	10.8 g/m	swirl	Fired outside-in
5017	0.35	32.4	10.8 g/m	swirl	Fired outside-in
5018	0.18	8.2	10.8 g/m	cross	2–8.2 m lengths
5019	0.26	12.2	10.8 g/m	cross	2–12.2 m lengths
5020	0.35	16.2	10.8 g/m	cross	2–16.2 m lengths
5021	1.39	16.4	85 g/m	swirl	Fired inside-out
5022	1.73	20.4	85 g/m	swirl	Fired inside-out
5023	2.75	32.4	85 g/m	swirl	Fired inside-out
5024	1.39	16.4	85 g/m	swirl	Fired outside-in
5025	1.73	20.4	85 g/m	swirl	Fired outside-in
5026	2.75	32.4	85 g/m	swirl	Fired outside-in

Bandwidths for Poulter and detonating cord sources were typically in the 50–150 Hz range. The detonating cord shots were lower amplitude but tended to have a slightly wider bandwidth (Figs. 3, 4). The lower amplitude may be partially caused by the typically smaller amounts of explosive used in the detonating cord sources.

We estimate penetration depth of the Poulter and detonating cord sources based on overall travel path length observed in reflection multiples (Fig. S1, S2). The penetration depth may vary based on the properties of the intraglacial and subglacial layers, their impedance contrast, and quality factor, so we are only able to provide rough estimates. The bed reflection multiple arrives at ∼3.5 seconds. Assuming a vertical travel path and an average velocity in ice of 3800 m/s, the total path length would be ∼13.3 km effective propagation in ice (Diez, 2014).

We compare the similarity of wavelets for P-waves (Fig. 5) and bed reflections (Fig. 6) recorded on the 24 seismic nodes for all of the different types of shots detonated at shotpoint 1 (Tables 1–3). In Figures 5–6, the amplitudes for each shot are normalized in order to see the wavelets better. Figure S5 shows the same data as Figure 5 without amplitude normalization, including Poulter shots, 5001–5009, detonating cord shots, 5010 to 5026, and shallowly drilled shot 5053. Configuration details for each shot are detailed in Tables 1–3. All incoming P-wave arrivals consist of a negative amplitude pulse followed by a positive amplitude pulse. Waveforms are generally simple, but Poulter shots 5001, 5002, 5003, and 5004 have a double positive pulse after the initial single pulse. Those sources were the Poulter shots with explosives elevated at 2.44 m, so the more complex recorded wavelets may be related to the height of the explosives; by contrast, Poulter shots with explosives elevated at 1.83 m appear to produce a cleaner wavelet. Plots without amplitude normalization (Fig. S5) clearly show that the Poulter shots have significantly higher amplitudes compared to the detonating cord shots, as expected from the total explosive detonated at each location (Tables 1–3). Only slight differences in wavelet and amplitude are seen for shots 5005 or 5006 (both 5 kg dynamite at 1.83 m) (Fig. 5, S5). Shot 5007 (2.5 kg dynamite at 1.83 m) with a smaller amount of explosive produces a lower amplitude P-wave, as expected (Fig. S5). Shot

https://doi.org/10.1017/jog.2024.41 Published online by Cambridge University Press

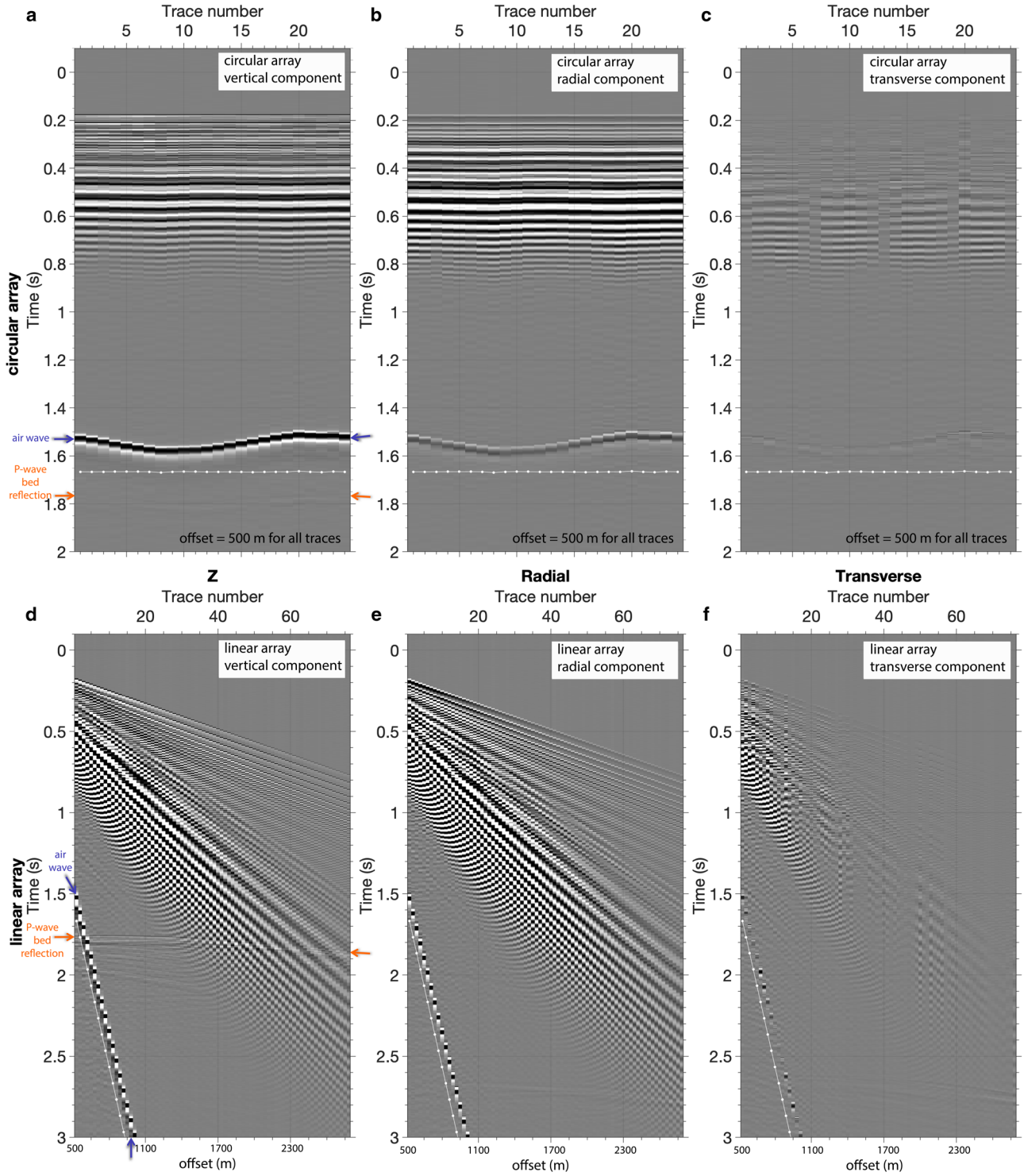

Figure 3. Shot gather recorded in three components on array 2 (circle of 24 nodes) (a, b, c) and array 1 (line of 75 nodes) (d, e, f) for Poulter shot 5004, 10 pentolite, 400-gram boosters taped to wood, suspended at ~2.44 meters above the ice, detonated at shot point 1. DC amplitude is removed to make the mean amplitude of each shot zero. Recorded horizontal components are rotated into radial and transverse components. The white line is the theoretical air wave.

5008 (5 kg emulsion +400 g pentolite booster at 1.83 m) has a similar amplitude to shot 5006 (5 kg dynamite at 1.83 m) (Fig. S5). However, shot 5009 (4 kg total: 10 400 g pentolite booster at 1.83 m) has a cleaner signal and higher amplitude (Fig. 5, S5). For the Poulter shots, we conclude that the preferred explosive is the pentolite booster, and a height of 1.83 m is preferred to 2.44 m.

Recordings on the circle of 24 seismic nodes of the detonating cord line parallel to the receiver line (shot 5010) and the detonating cord line perpendicular to the receiver line (shot 5011) demonstrate the anisotropy of the radiation pattern of waves generated by linear detonating cord shots (Fig. 5, S5). The detonating cord crosses (shots 5018–5020) have more isotropic wave propagation, as observed by the circle of 24 nodes (Fig. 5, S5).

Comparing detonating cord swirls with 85 g/m and various lengths and diameters of the swirls, shot 5021 (16.4 m of cord in a swirl with 3 m diameter) looks similar to shot 5022 (20.4 m of cord in a swirl with 3.5 m diameter) and shot 5023 (32.4 m of cord in a swirl with 4 m diameter) (Fig. 5, S6). The larger lengths of cord and higher diameters of swirl appear to

https://doi.org/10.1017/jog.2024.41 Published online by Cambridge University Press

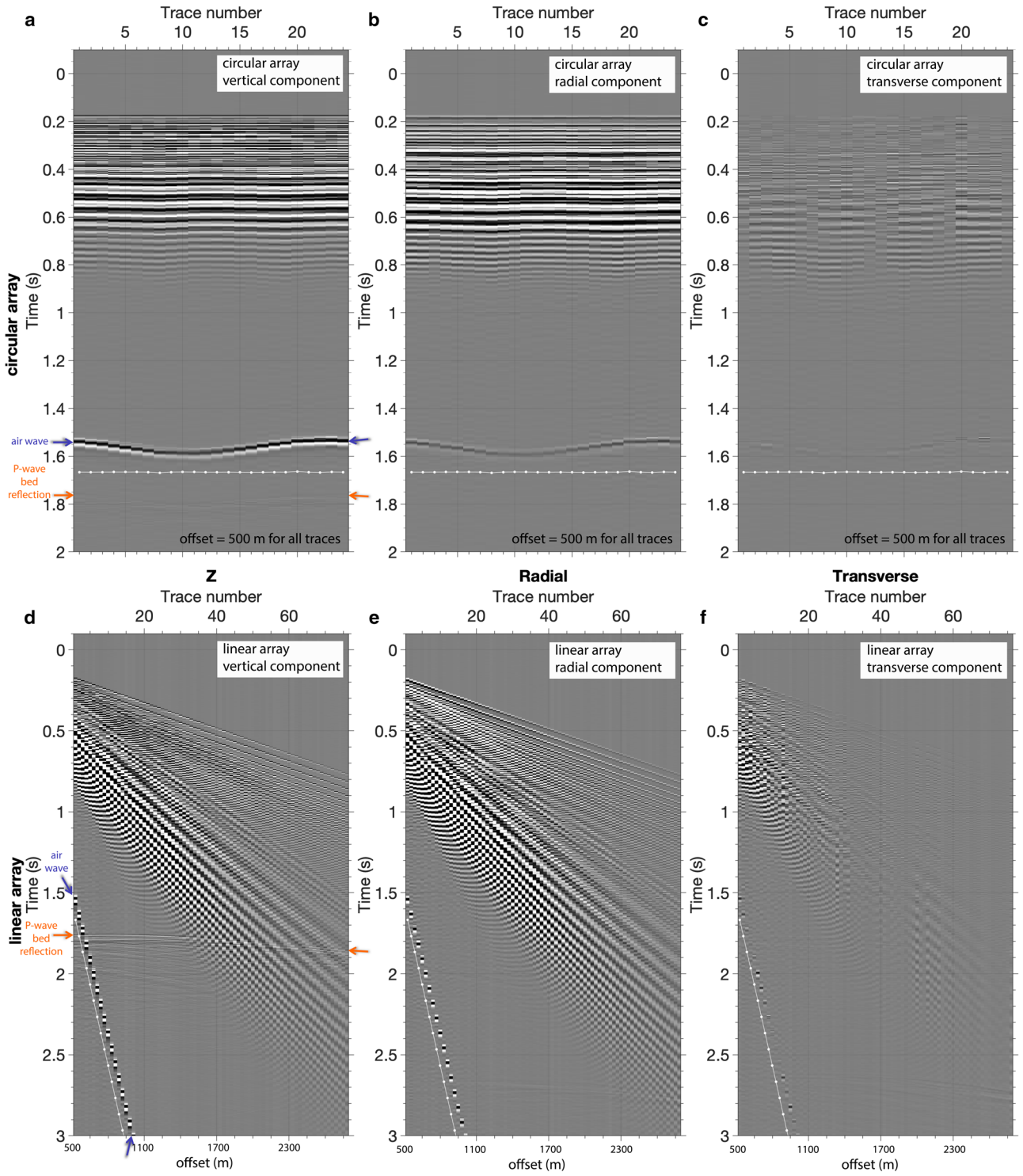

Figure 4. Shot gather recorded in three components on array 2 (circle of 24 nodes) (a, b, c) and array 1 (line of 75 nodes) (d, e, f) for detonating cord shot 5026, a swirl using 32.4 m 85 g/m fired inside-out with 4 m diameter, 2.75 kg explosives, detonated at shot point 1. DC amplitude is removed to make the mean amplitude of each shot zero. Recorded horizontal components are rotated into radial and transverse components. The white line is the theoretical air wave.

correspond to progressively lower amplitudes (Fig. S5, S7). This is true at all frequencies (Fig. 7). Having a more tightly coiled detonating cord shot seems to improve the signal generation. For the 10.8 g/m detonating cord, 5014 (32.4 m of cord in a swirl with 4 m diameter) appears slightly higher amplitude than 5012 (20.4 m of cord in a swirl with 3.5 m diameter) and 5013 (16.4 m of cord in a swirl with 3 m diameter) (Fig. S5, S7).

Compared to the Poulter and detonating cord shots, shot 5053, the shallowly drilled shot with two 0.15 kg pentolite boosters installed at 3.1 meters depth, has a generally lower signal to noise ratio and a more complex waveform source (Fig. 5, S4, S5). Part of the reason might be the smaller amount of explosive (300 g total compared to 180 g to 5.4 kg for the other sources), but the detonating cord shots with a similar amount of explosive (5014, 5017, 5019, 5020) generally have cleaner signals (Fig. 5) with a slightly higher amplitude (Fig. S5). We also observe a signal following the first arriving P-wave that might be the ghost arrival from the reflected P-wave off the snow surface (Fig. S4). Thus we conclude that Poulter and detonating cord surface shots are preferable to shallow drilled and loaded shots.

https://doi.org/10.1017/jog.2024.41 Published online by Cambridge University Press

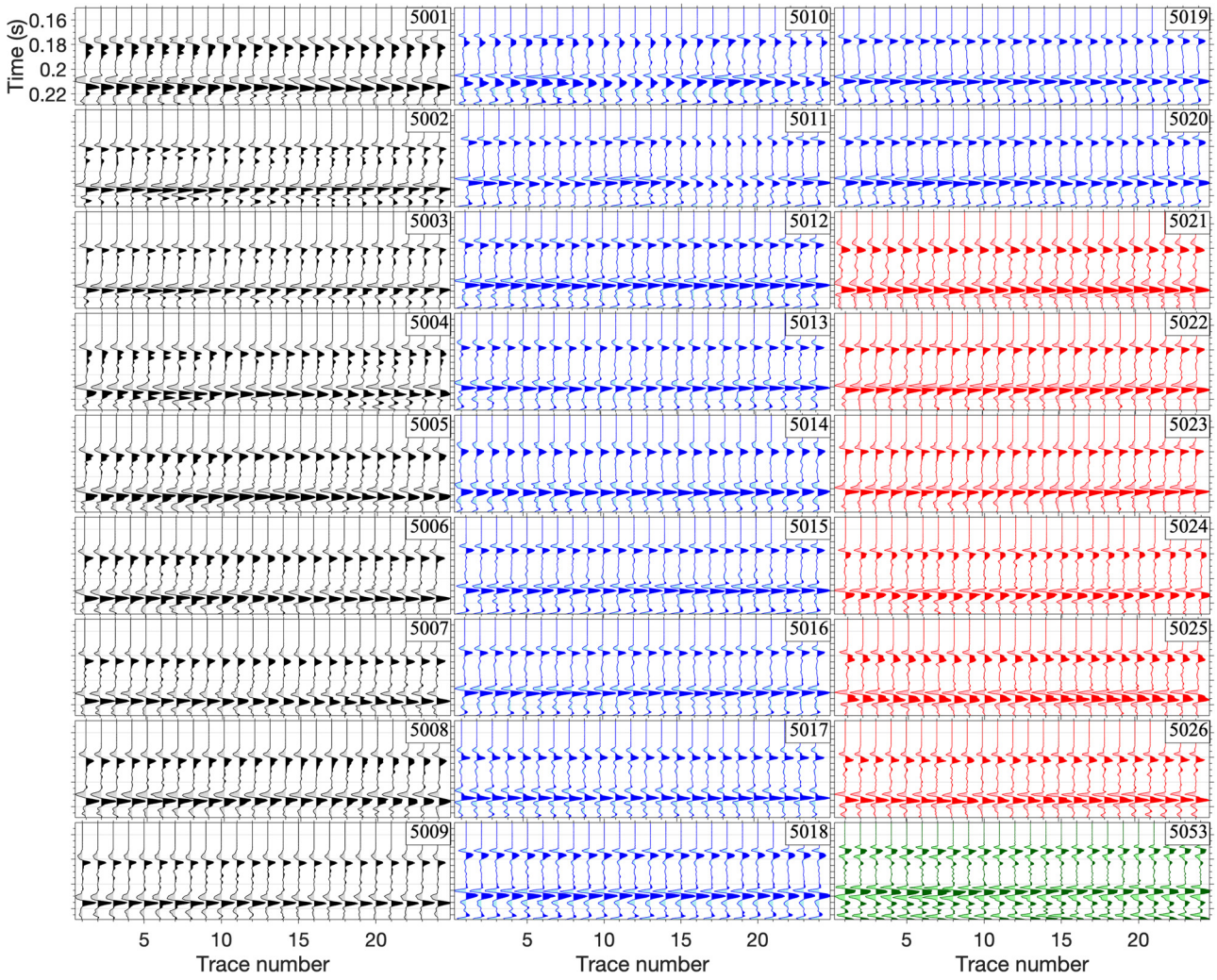

Figure 5. Plots showing vertical component waveforms for first arriving waves recorded on the 24 seismic nodes in the circle for all of the different types of sources detonated at shotpoint 1 in order to compare wavelet similarity. Amplitudes are normalized for each shot, so amplitudes cannot be compared between different shot points. DC amplitude is removed to make the mean amplitude of each shot zero. 5001–5009 are Poulter shots. 5010 to 5020 are 10.8 g/m detonating cord shots. 5021–5026 are 85 g/m detonating cord shots. 5053 is a shallowly drilled shot. Configuration details for each shot are detailed in Tables 1–3. Figure S4 shows the same data without amplitude normalization. Waveforms for Poulter shots are colored black, for 50 grains/ ft detonating cord are red, for 400 grains/ ft detonating cord are blue, and for the drilled 300 g pentolite shot are colored green. For each shot, traces are ordered by seismic node number in the circle, from 1–24.

Amplitude spectra for direct P, S, air, and reflected waves recorded on the 24 seismic nodes in the circle for all of the different types of shots detonated at shotpoint 1 are shown in Figure 7. Configuration details for each shot are detailed in Tables 1–3. Spectra clearly show that the Poulter shots (5001–5009) are richer in lower frequency signals ($\sim 10-20$ Hz) compared to the detonating cord shots (5010–5026) and the shallowly-drilled shot (5053). Detonating cord shots are richer in high frequency signals (>20 Hz) (Fig. 7). Eighty-five g/m detonating cord produces lower frequency signals compared to the 10.8 g/m detonating cord. The shallow drilled shot contains mostly higher frequency (>60 Hz) signals, with lower amplitudes for frequencies <60 Hz compared to the detonating cord or the Poulter sources. Frequency content is also affected by detonation velocity, which varies between sources used here.

Amplitude spectra for whole traces and reflected waves also show clearly that the Poulter shots are stronger at low frequencies and comparable at high frequencies relative to the thicker detonating cord (85 g/m) (Fig. 8). Thinner detonating cord (10.8 g/m) has weaker signals at all frequencies compared to the Poulter shots, but the shallowly-drilled, 300 g shot is the weakest at all frequencies (Fig. 7). The same observations are true of the whole waves and the reflected waves (Fig. 8). Whole waves include time 0 to 2.05 seconds, and reflected waves include time 1.7 to 1.9 seconds. Figures 3 and 4 and S4 show example shot gathers including times.

One of the challenges observed with all of the explosive surface sources (due to their detonation on top of a relatively thick firn layer) is the generation of coherent noise (seen in Fig. 3, 4, and S4). While this noise may have a distinct signature in the frequency-wavenumber domain, it can be difficult to filter and may require front muting. This type of noise is usually stronger for surface or shallow shots compared to deeper buried shots when there is a surface firn layer. An additional challenge of the Poulter shots is that they require large shot charges (5–8 times larger than the equivalent shots drilled at >20 meters). Poulter shots save the weight of the hot water drill but typically require a larger weight of explosives.

4. Directivity of detonating cord shots

Shooting a detonating cord swirl inside-out versus outside-in appears to cause slight differences in the wavelets recorded by the circle of nodes. In addition, the outside-in shots appear to

https://doi.org/10.1017/jog.2024.41 Published online by Cambridge University Press

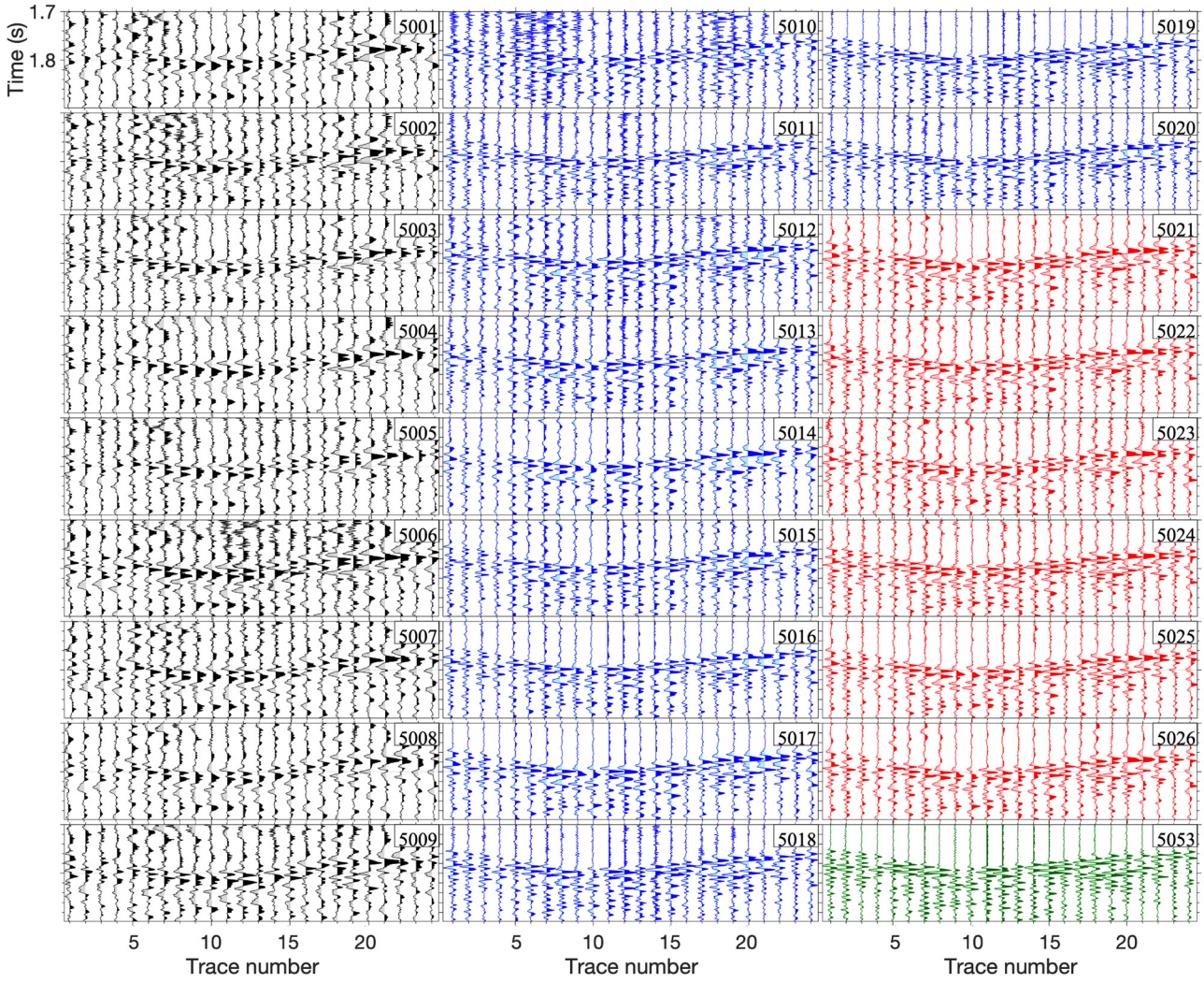

Figure 6. Plots showing vertical component waveforms for bed reflections recorded on the 24 seismic nodes in the circle for all of the different types of sources detonated at shotpoint 1 in order to compare wavelet similarity. Amplitudes are normalized for each shot, so amplitudes cannot be compared between different shot points. DC amplitude is removed to make the mean amplitude of each shot zero. 5001–5009 are Poulter shots. 5010 to 5020 are 10.8 g/m detonating cord shots. 5021–5026 are 85 g/m detonating cord shots. 5053 is a shallowly drilled shot. Configuration details for each shot are detailed in Tables 1–3. Waveforms for Poulter shots are colored black, for 50 grains/ ft detonating cord are red, for 400 grains/ ft detonating cord are blue, and for the drilled 300 g pentolite shot are colored green. For each shot, traces are ordered by seismic node number in the circle, from 1–24.

result in a higher recorded amplitude on the circle of nodes compared to the inside-out detonating cord shots (Fig. S5, S7). Shots 5014 and 5017 are both 32.4 m of cord arranged in a swirl with 4 m diameter, fired inside-out and outside-in, respectively, and they have slightly different waveforms (Fig. 5, S6) with larger amplitudes for shot 5017 (Fig. S5, S7). Similarly, comparing the pairs of other detonating cord shots fired inside-out and outside-in shows a similar pattern (Fig. 5, S5, S6, S7). The pairs of inside-out followed by outside-in shots of the same length and diameter for the 85 g/m cord are: (1) 5021 and 5024 (16.4 m length and 3 m diameter), (2) 5022 and 5025 (20.4 m length and 3.5 m diameter), and (3) 5023 and 5026 (32.4 m length and 4 m diameter) (Fig. S6 and S7). The pairs of inside-out followed by outside-in shots of the same length and diameter for the 10.8 g/m cord are: (1) 5012 and 5015 (16.4 m length and 3 m diameter), (2) 5013 and 5016 (20.4 m length and 3.5 m diameter), and (3) 5014 and 5017 (32.4 m length and 4 m diameter) (Fig. S6, S7). Shooting detonating cord outside-in appears to yield more high frequency energy from ~70 – 130 Hz compared to shooting inside-out (Fig. 7). Shooting outside-in also appears to result in higher amplitudes for waves recorded by the circle of nodes (Fig. S5, S7). We conclude that shooting outside-in produces a better signal for seismic imaging (both frequency and amplitude) than shooting inside-out.

Table 3. Description of shallowly-drilled explosive source at shotpoint 1

Shot ID	Weight (kg)	Depth (m)	Type	Description
5053	0.3	3.1	Pentolite booster	2–0.15 kg booster

5. Logistical considerations and recommendations for 2-D and 3-D seismic surveys

The Poulter shots required less time and effort to set up compared to the detonating cord shots. For the Poulter shots, the explosives and detonator were taped to the top of an approximately 1 m long piece of 1.27 by 1.91 cm sacrificial wood, and then the wood was connected to the top of the metal shot pole. The set-up took approximately 10 minutes per shot and required little physical effort. The detonating cord had to be cut from the spool to the appropriate length and then arranged in the snow. The linear arrays took less time to arrange than the swirls with one person laying the detonating cord in the snow and another person

https://doi.org/10.1017/jog.2024.41 Published online by Cambridge University Press

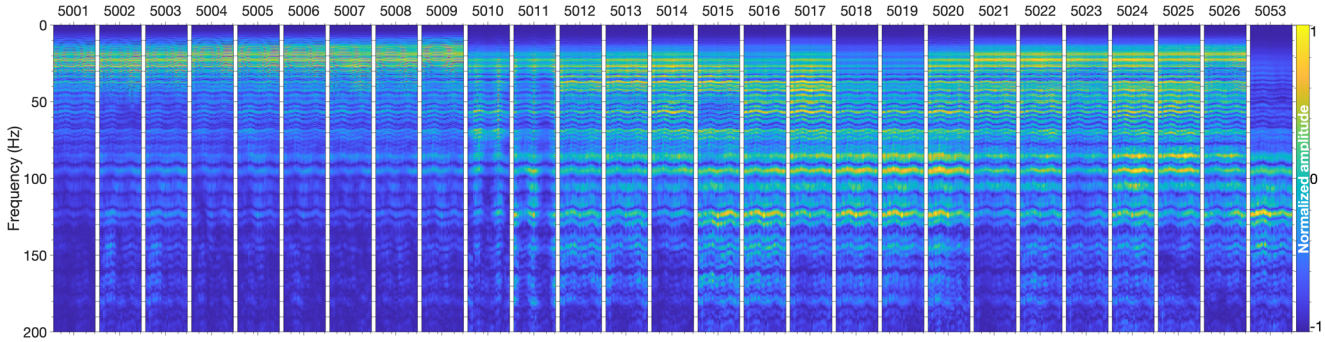

Figure 7. Amplitude spectra showing amplitude for each frequency for a time window including the direct P, S, air, and reflected waves (time 0 to 2.05 seconds, as shown in Figs. 3 and 4) recorded on the vertical component of the 24 seismic nodes in the circle for all of the different types of shots detonated at shotpoint 1. Amplitude is normalized for each shot. 5001–5009 are Poulter shots. 5010 to 5026 are detonating cord shots. 5053 is a shallowly drilled shot. Configuration details for each shot are detailed in Tables 1–3.

following behind to cover the cord with snow to weigh it down and improve coupling to the snow surface. The longer 32.4 m lines took about 15 minutes to cut, lay down, wire to the detonator, and cover with snow. The larger swirls of 32.4 meters took nearly 30 minutes to cut, lay down in a swirl, and cover with snow, largely because the detonating cord had a tendency to curl and would not lay down flat until snow weighed it down.

Future 2-D and 3-D seismic surveys will benefit from large numbers of seismic sources, to improve the fold (number of reflection samples per bin), increase resolution of imaging, increase the azimuth of recording, and increase the physical area that is imaged. The field effort and time required when wiring and detonating more than 25 shots in a day was significantly more for the detonating cord swirls than for the Poulter shots. However, the detonating cord linear configurations required only slightly more time per shot compared to the Poulter shots. Both Poulter shots and detonating cord linear configurations can be set up and detonated in 6–7 minutes, once the procedure is streamlined. Of course, drilled and loaded shots require the least time to detonate once they are drilled, loaded, and wired in the ice, but significantly more time and effort is expended in the drilling and loading stages. For the shallowly drilled and loaded shot presented in this paper, the 3–4 meter drilled shot hole took about 20 mins to drill and load. As described above, the data quality was not as good for the shallow drilled shot. A single 40 m drilled shot hole is likely to take more than one hour to drill and transport the drill to the next site. Drilling to 40 m depth in ice also requires specialized drilling equipment that weighs more than 500 kg. Drilling to 20–25 meters depth may take as little as 20 minutes per hole, but there is also time for loading and stemming the hole and for the drill set up and overnight storage time. Surface explosive sources provide a useful alternative for many projects, especially imaging projects that require numerous sources, such as large 3-D surveys, in remote

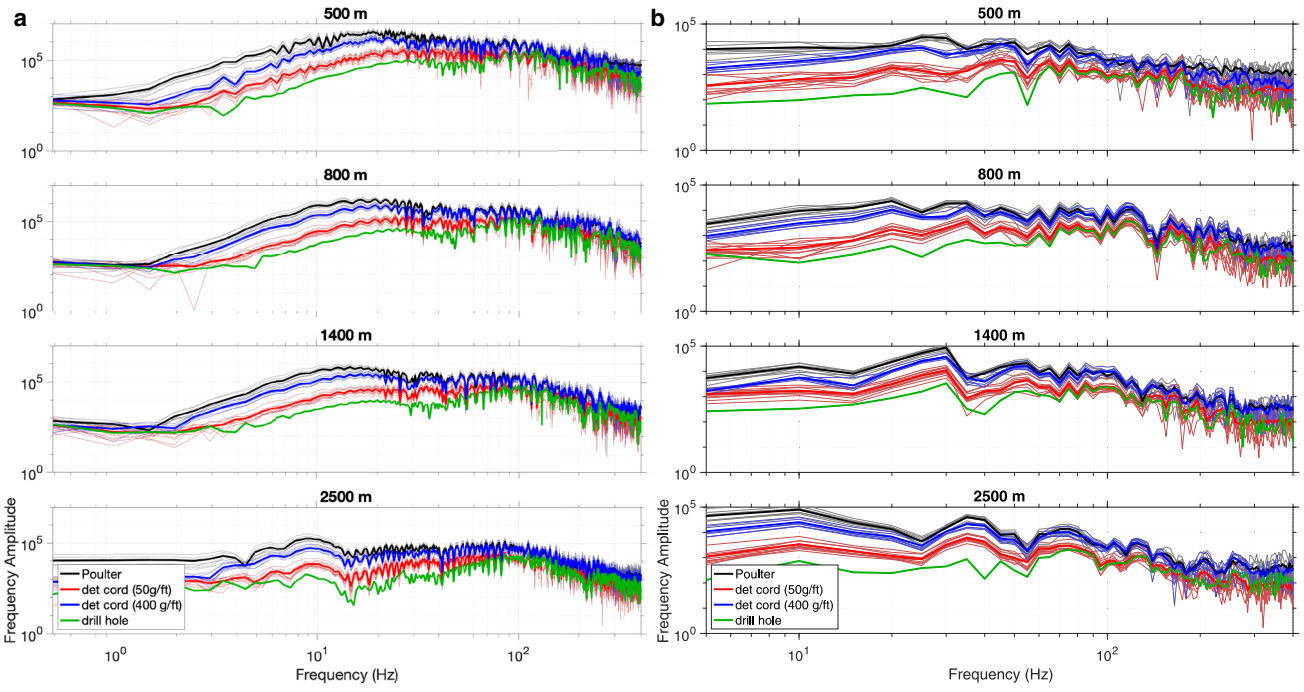

Figure 8. Comparison of amplitude spectra for (a) the whole traces (time 0 to 2.05 seconds) and (b) the reflected waves (time 1.7 to 1.9 seconds). Example shot gathers showing times are shown in Figures 3–4. Colors indicate different shot types: Poulter (black), detonating cord (50 grains/ ft; red), detonating cord (400 grains/ ft; blue), drilled shot (green). The Poulter shots are stronger for low frequencies and comparable at high frequencies relative to the thicker detonating cord. The thinner detonating cord is less strong at all frequencies, and the shallowly-drilled, 300 g shot is the weakest at all frequencies. Bold lines are the average frequency amplitude for each shot type.

https://doi.org/10.1017/jog.2024.41 Published online by Cambridge University Press

areas or complicated terrain where time, cargo, personnel and/ or accessibility are limited. We found the Poulter shots to be the best choice for optimizing the time and physical effort needed to set up and detonate the shots.

6. Conclusions

Controlled-source shot tests near the West Antarctic Ice Sheet Divide Camp allow us to compare Poulter shots (where explosives are suspended on a pole and detonated above the Earth's surface), surface detonating cord shots, and shallowly-drilled shots at ∼3 meters depth. We compare Poulter shots of various sizes, explosive types, and heights above the snow surface. We compare detonating cord shots of various cord weights (10.8 g/m and 85 g/m), cord lengths, cord configurations (swirl, cross, line), and detonation pattern (shooting inside-out versus outside-in). We observe that Poulter shots have lower frequencies and generally higher amplitudes than the detonating cord shots, perhaps because they used a larger weight of explosive material. The detonating cord shots have higher amplitudes than the shallowly-drilled shot. Poulter shots at 1.83 m height above snow surface resulted in a cleaner waveform compared to Poulter shots at 2.44 m height above snow surface. Of the dynamite, emulsion, and pentolite booster explosive types used for Poulter shots, the pentolite booster had the cleanest and strongest signal. Shooting a detonating cord swirl outside-in appeared to improve both frequency and amplitude of recorded seismic signals compared to shooting inside-out. We conclude from these tests that Poulter shots are a better choice than detonating cord, offering signals that are richer in lower frequencies and with no compromise to high frequency content. Poulter shots were also less labor intensive compared to detonating cord shots or shallowly drilled shots using our work flow.

Supplementary material. The supplementary material for this article can be found at https://doi.org/10.1017/jog.2024.41

Acknowledgements. The WAIS Divide data is from the Thwaites Interdisciplinary Margin Evolution (TIME) project, a component of the International Thwaites Glacier Collaboration (ITGC). Support from National Science Foundation (NSF: Grant 1739027) and Natural Environment Research Council (NERC: Grant NE/S006788/1). Logistics provided by NSF-U.S. Antarctic Program and NERC-British Antarctic Survey. ITGC Contribution No. ITGC121.

The seismic instruments were provided by EarthScope Consortium through the PASSCAL Polar Support Services. Data collected will be available through EarthScope. The facilities of EarthScope Consortium are supported by the National Science Foundation's Seismological Facility for the Advancement of Geoscience (SAGE) Award under Cooperative Support Agreement OPP-1851037. Geodetic instruments were provided by the GAGE Facility, operated by EarthScope Consortium, with support from the National Science Foundation, the National Aeronautics and Space Administration, and the U.S. Geological Survey under NSF Cooperative Agreement EAR-1724794.

We thank Leslie Blank, James King, the U.S. Air National Guard, and Kenn Borek Air for logistical support. We thank Nick Gillette, Andrew Lloyd, Sridhar Anandakrishnan, Kiya Riverman, and the camp staff of WAIS Divide for their field assistance and support. Finally, we are grateful for comments from Coen Hofstede, an anonymous reviewer, and the editor, Bernd Kulessa, that improved the manuscript.

References

Battle MO and 8 others (2011) Controls on the movement and composition of firn air at the West Antarctic ice sheet divide. *Atmospheric Chemistry and Physics* **11**(21), 11007–11021. doi: 10.5194/acp-11-11007-2011

Bentley C (1972) Seismic-wave velocities in anisotropic ice: a comparison of measured and calculated values in and around the deep drill hole at Byrd station, Antarctica. *Journal of Geophysical Research* **77**, 4406–4420. doi: 10.1029/JB077i023p04406

Bentley C and Ostenso N (1961) Glacial and subglacial topography of West Antarctica. *Journal of Glaciology* **3**(29), 882–911.

Blankenship D, Bentley C, Rooney S and Alley R (1987) Till beneath ice stream b: 1. properties derived from seismic travel times. *Journal of Geophysical Research: Solid Earth* **92**(B9), 8903–8911.

Booth A and 6 others (2012) Thin-layer effects in glaciological seismic amplitude-versus-angle (ava) analysis: implications for characterising a subglacial till unit, russell glacier, West Greenland. *The Cryosphere* **6**, 909–922. doi: 10.5194/tc-6-909-2012

Booth AD and 5 others (2013) A comparison of seismic and radar methods to establish the thickness and density of glacier snow cover. *Annals of Glaciology* **54**(64), 73–82. doi: 10.3189/2013AoG64A044

Chaput J, Aster R, Karplus M and Nakata N (2022a) Ambient high frequency seismic surface waves in the firn column of central West Antarctica. *Journal of Glaciology* **68**, 785–798. doi: 10.1017/jog.2021.135

Chaput J and 8 others (2022b) Near-surface seismic anisotropy in Antarctic glacial snow and ice revealed by high frequency ambient noise. *Journal of Glaciology* 1–17. doi: 10.1017/jog.2022.98

Chaput J, Aster R and Karplus M (2023) The singing firn. *Annals of Glaciology* 1–6. doi: 10.1017/aog.2023.34

Conway H and Rasmussen L (2009) Recent thinning and migration of the western divide, central west Antarctica. *Geophysical Research Letters* **36**(12), L12502.

Diez A (2014) Effects of cold glacier ice crystal anisotropy on seismic data. *Ph.D. Dissertation, Alfred Wegener Institute.*

Diez A and 8 others (2015) Seismic wave propagation in anisotropic ice - part 2: Effects of crystal anisotropy in geophysical data. *The Cryosphere* **9**, 385–398. doi: 10.5194/tc-9-385-2015

Eisen O and 7 others (2015) On-ice vibroseis and snowstreamer systems for geoscientific research. *Polar Science* **9**, 51–65. doi: 10.1016/j.polar.2014.10.003

Greene C, Gwyther D and Blankenship D (2017) Antarctic mapping tools for matlab. *Computers and Geosciences* **104**, 151–157. doi: 10.1016/j.cageo.2016.08.003

Hofstede C and 10 others (2021) Evidence for a grounding line fan at the onset of a basal channel under the ice shelf of support force glacier, Antarctica, revealed by reflection seismics. *The Cryosphere* **15**(3), 1517–1535. doi: 10.5194/tc-15-1517-2021

Horgan H, Anandakrishnan S, Alley R, Burkett P and Peters L (2011) Englacial seismic reflectivity: imaging crystal-orientation fabric in West Antarctica. *Journal of Glaciology* **57**(204), 639–649.

Kaip G and 5 others (2018) West Antarctic ice sheet (wais) divide source testing. *International Federation of Digital Seismograph Networks.*

Kluskiewicz D and 5 others (2017) Sonic methods for measuring crystal orientation fabric in ice and results from west Antarctic ice sheet (wais) divide. *Journal of Glaciology* **63**(240), 603–617.

Kohnen H (1974) The temperature dependence of seismic waves in ice. *Journal of Glaciology* **13**, 144–147.

Luthra T, Anandakrishnan S, Winberry J, Alley R and Holschuh N (2016) Basal characteristics of the main sticky spot on the ice plain of Whillans ice stream, Antarctica. *Earth and Planetary Science Letters* **440**, 12–19.

Morlighem M and 36 others (2020) Deep glacial troughs and stabilizing ridges unveiled beneath the margins of the Antarctic ice sheet. *Nature Geoscience* **13**, 132–137. doi: 10.1038/s41561-019-0510-8

Pattyn F (1996) Numerical modelling of a fast-flowing outlet glacier: experiments with different basal conditions. *Annals of Glaciology* **23**, 237–246.

Peters L, Anandakrishnan S, Alley R and Voigt D (2012) Seismic attenuation in glacial ice: a proxy for englacial temperature. *Journal of Geophysical Research* **117**, F02008. doi: 10.1029/2011JF002201

Picotti S, Vuan A, Carcione J, Horgan H and Anandakrishnan S (2015) Anisotropy and crystalline fabric of Whillans ice stream (West Antarctica) inferred from multicomponent seismic data. *Journal of Geophysical Research: Solid Earth* **120**, 4237–4262. doi: 10.1002/2014JB011591

Pimentel S, Flowers G and Schoof G (2010) A hydrologically coupled higher-order flow-band model of ice dynamics with a coulomb friction sliding law. *Journal of Geophysical Research* **115**, F04023. doi: 10.1029/2009JF001621

Poulter T (1950) The poulter seismic method of geophysical exploration. *Geophysics* **15**(2), 181–207.

Ringler A, Anthony R, Karplus M, Holland A and Wilson D (2018) Laboratory tests of three z-land fairfield nodal 5-Hz, three-component sensors. *Seismological Research Letters* **89**, 1601–1608. doi: 10.1785/0220170236

Robin G (1953) Ii. summary of seismic shooting investigations in dronning maud land. *Journal of Glaciology* **2**, 205–211. doi: 10.3189/S0022143000025740

Roethlisberger H (1972) Seismic exploration in cold regions. *Science Engineering Monograph II-A2a*.

Sen V and 5 others (1998) Seismic surveys in central West Antarctica: data and processing examples from the antalith field tests (1994–1995). *Terra Antarctica* **5**(4), 761–772.

Sergienko O and Hulbe C (2011) 'Sticky spots' and subglacial lakes under ice streams of the siple coast, Antarctica. *Annals of Glaciology* **52**, 18–22.

Truffer M, Echelmeyer K and Harrison W (2001) Implications of till deformation on glacier dynamics. *Journal of Glaciology* **47**, 123–134. doi: 10.3189/172756501781832449

Veitch S and 5 others (2021) Ice thickness estimates of lemon creek glacier, from active-source seismic imaging. *Journal of Glaciology* **0**, 1–9. doi: 10.1017/jog.2021.32

Young T and 5 others (2021) Rapid and accurate polarimetric radar measurements of ice crystal fabric orientation at the Western Antarctic ice sheet (wais) divide ice core site. *The Cryosphere* **15**, 4117–4133. doi: 10.5194/tc-15-4117-2021

Zhang Z, Nakata N, Karplus M, Kaip G and Yi J (2022) Shallow ice-sheet composite structure revealed by seismic imaging near the west Antarctic ice sheet (wais) divide camp. *Journal of Geophysical Research: Earth Surface* **127**, e2022JF006777. doi: 10.1029/2022JF006777

https://doi.org/10.1017/jog.2024.41 Published online by Cambridge University Press